ARTICLE
Journal of Cellular Biochemistry 113:1190–1197 (2012)

Journal of Cellular Biochemistry

Mutagenesis Studies of the β I Domain Metal Ion Binding Sites on Integrin αVβ3 Ligand Binding Affinity

Joel Raborn and Bing-Hao Luo*

Department of Biological Sciences, 202 Life Sciences Building, Louisiana State University, Baton Rouge, Louisiana 70803

ABSTRACT

Three divalent cation binding sites in the integrin β I domain have been shown to regulate ligand binding and adhesion. However, the degree of ligand binding and adhesion varies among integrins. The αLβ2 and α4β7 integrins show an increase in ligand binding affinity and adhesion when one of their ADMIDAS (adjacent to MIDAS, or the metal ion-dependent adhesion site) residues is mutated. By contrast, the α2β1, α5β1, and αIIbβ3 integrins show a decrease in binding affinity and adhesion when their ADMIDAS is mutated. Our study here indicated that integrin αVβ3 had lower affinity when the ADMIDAS was mutated. By comparing the primary sequences of these integrin subunits, we propose that one residue associated with the MIDAS (β3 Ala^{252}) may account for these differences. In the β1 integrin subunit, the corresponding residue is also Ala, whereas in both β2 and β7 integrin subunits, it is Asp. We mutated the β3 residue Ala^{252} to Asp and combined this mutant with mutations of one or two ADMIDAS residues. The mutant A252D showed reduced ligand binding affinity and adhesion. The ligand binding affinity and adhesion were increased when this A252D mutant was paired with mutations of one ADMIDAS residue. But when paired with mutations of two ADMIDAS residues the mutant nearly abolished ligand-binding ability, which was restored by the activating glycosylation mutation. Our study suggests that the variation of this residue contributes to the different ligand binding affinities and adhesion abilities among different integrin families. J. Cell. Biochem. 113: 1190–1197, 2012.

KEY WORDS: INTEGRIN; METAL ION BINDING SITES; CONFORMATIONAL CHANGE; CELL SPREADING; GLYCOSYLATION

Binding of the heterodimeric cell-adhesion integrins to their respective ligands is regulated by divalent cations [Mould et al., 1995, 2003b; Hynes, 2002; Chen et al., 2003, 2004; Luo et al., 2007]. Normally, Ca^{2+} stabilizes the low affinity state, whereas some divalent cations such as Mn^{2+} can activate integrins for ligand binding. Nearly half of the known integrins contain an α I domain, which is the site of ligand binding for these integrins. However, for integrins lacking this α I domain such as the β3 family, ligands bind to the β I domain [Lee et al., 1995; Xiong et al., 2001, 2002; Shimaoka et al., 2002, 2003; Takagi et al., 2003; Xiao et al., 2004]. This β I domain contains three metal ion-coordinating sites responsible for ligand binding affinity and adhesion. First, the metal ion-dependent adhesion site (MIDAS) is in the center, with the synergistic metal binding site (SyMBS) and the adjacent to MIDAS (ADMIDAS) on either side [Lee et al., 1995; Hynes and Zhao, 2000; Harding, 2001; Whittaker and Hynes, 2002; Xiong et al., 2002; Chen et al., 2003, 2004; Shimaoka et al., 2003; Mould et al., 2003a; Xiao et al., 2004; Zhu et al., 2008].

The β I domain MIDAS appears to be required for ligand binding. In the β3 family of integrins, the DXSXS motif of the MIDAS coordinates with Mg^{2+} in normal physiological conditions [Xiao et al., 2004; Zhu et al., 2008]. According to previous reports, the Asp carboxyl group of the RGD motif of the ligand coordinates with the MIDAS Mg^{2+} ion that stabilizes the ligand–integrin interaction during ligand binding [Xiong et al., 2002; Xiao et al., 2004]. In mutagenesis studies involving the MIDAS, the ligand binding affinity is subsequently abolished, which suggests the importance of the MIDAS for ligand binding [Loftus et al., 1990; Goodman and Bajt, 1996; Tozer et al., 1996; Lin et al., 1997; Chen et al., 2003; Valdramidou et al., 2008]. The SyMBS borders the MIDAS and coordinates Ca^{2+}. The β3 SyMBS residue Glu^{220} coordinates with low concentrations of Ca^{2+} and the MIDAS Mg^{2+} to assist ligand binding, consequently acting as an allosteric activator for ligand binding [Xiao et al., 2004; Zhu et al., 2008]. Mutations in this site have revealed that the SyMBS is important but not required for ligand binding, although the exact biological role of the SyMBS

Grant sponsor: American Heart Association; Grant number: #10GRNT3960011; Grant sponsor: Louisiana Board of Regents; Grant number: LEQSF(2009-12)-RD-A07.

*Correspondence to: Bing-Hao Luo, Department of Biological Sciences, 202 Life Sciences Building, Louisiana State University, Baton Rouge, LA 70803. E-mail: luo@lsu.edu

Received 29 September 2011; Accepted 3 November 2011 • DOI 10.1002/jcb.23448 • © 2011 Wiley Periodicals, Inc.
Published online 17 November 2011 in Wiley Online Library (wileyonlinelibrary.com).

remains elusive [Kamata et al., 2002; Chen et al., 2003, 2004, 2006; Salas et al., 2004; Murcia et al., 2008; Valdramidou et al., 2008; Raborn et al., 2011]. Furthermore, the ADMIDAS is located on the opposite side of the MIDAS and coordinates Ca^{2+} [Chen et al., 2003, 2006; Mould et al., 2003a; Valdramidou et al., 2008]. In the closed headpiece conformation, the carbonyl backbone of β3 Met^{335} associates with the ADMIDAS Ca^{2+} ion. When the integrin undergoes inside-out activation, the hybrid domain swings out, causing a downward displacement of the α7 helix and consequently severing the interaction between Met^{335} and the Ca^{2+} ion [Takagi et al., 2002; Luo et al., 2004, 2009; Xiao et al., 2004; Yang et al., 2004; Chen et al., 2006]. In the high affinity open headpiece conformation, Asp^{251} moves toward the ADMIDAS ion. The carboxyl group of Asp^{251} associates with the ADMIDAS Ca^{2+} ion. This shift inadvertently makes the MIDAS more positive able to bind ligands with a higher affinity [Zhu et al., 2008]. Mutagenesis studies have confirmed that the ADMIDAS stabilizes both the low affinity closed headpiece and the high affinity open headpiece confirmations [Zhu et al., 2008; Raborn et al., 2011].

Differences in ligand binding affinity and adhesion ability exist among integrins [Bajt and Loftus, 1994; Chen et al., 2003, 2004; Mould et al., 2003a; Valdramidou et al., 2008]. Previous mutagenesis studies of the ADMIDAS have shown conflicting results [Chen et al., 2003, 2004, 2006; Mould et al., 2003a; Valdramidou et al., 2008; Raborn et al., 2011]. In studies with α4β7 and αLβ2, mutations in the ADMIDAS increase ligand binding and firm adhesion compared to the WT [Chen et al., 2003, 2004, 2006]. By contrast, studies of the α2β1, α5β1, and αIIbβ3 integrins showed that ADMIDAS mutations decreased ligand binding and adhesion [Mould et al., 2003a; Valdramidou et al., 2008; Raborn et al., 2011]. In this study, we showed that ADMIDAS mutations of integrin αVβ3 also decreased ligand binding. The reason for the discrepancies among different integrin families remains unknown. Interestingly, these integrins differ in a specific residue associated with the MIDAS, namely the β3 residue Ala^{252}. The corresponding residue in the β1 integrin subunit is also Ala, whereas it is Asp in the β2 and β7 integrin subunits. Here, we introduced a mutation in the αVβ3 to covert this MIDAS associated Ala^{252} to Asp. By combination of this mutant with mutations of one or two ADMIDAS residues, we studied the effects of this residue on ligand binding and adhesion. We found that the variation in this MIDAS associated residue accounts for the differences in ligand binding and adhesion among different integrins, and it also accounts for the conflicting results of ADMIDAS mutations within different integrins. Interestingly, an activating glycosylation mutation, introduced into the αV lower leg to disrupt the αβ association, was able to restore the ligand binding affinity and adhesion ability of these mutants. This study provides insight into the role of this MIDAS associated residue in regulating ligand binding and adhesion.

MATERIALS AND METHODS

PLASMID CONSTRUCTION AND EXPRESSION

Plasmids with sequences for full-length human αV and β3 were subcloned into pEF/V5-HisA and pcDNA3.1/Myc-His (+), respectively [Takagi et al., 2002; Luo et al., 2003]. The αV mutant E781N/R783T and the β3 mutants D127A, D126A/D127A, A252D, A252D/D127A, and A252D/D126A/D127A were made using site-directed mutagenesis with the QuikChange kit (Stratagene, La Jolla, CA). Constructs were transfected into HEK293T cells (American Type Culture Collection, Manassas, VA) using a FuGENE transfection kit (Roche Applied Science, Indianapolis, IN) according to the manufacturer's instructions. The expression levels of αV and β3 were detected by flow cytometry staining with the following monoclonal antibodies: AP3 (nonfunctional anti-β3 mAb, American Type Culture Collection), 7E3 (anti-β3 mAb), LM609 (anti-αV mAb), and 10E5 (anti- αIIb mAb, kindly provided by B. S. Coller, Rockefeller University, New York, NY).

TWO-COLOR LIGAND BINDING ASSAY ON HEK293T TRANSFECTANTS

Soluble binding of Alexa Fluor 488-labeled human fibrinogen and fibronectin (Enzyme Research Laboratories, South Bend, IN) was determined as previously described [Luo et al., 2003]. Briefly, transfected cells suspended in 20 mM HEPES-buffered saline, pH 7.4 (HBS) supplemented with 5.5 mM glucose, and 1% bovine serum albumin (BSA) were incubated on ice for 30 min with 60 μg/ml fibrinogen or 60 μg/ml fibronectin in the presence of either 5 mM EDTA, 5 mM Ca^{2+}, or 1 mM Mn^{2+}. Cells were also stained in parallel with Cy3-conjugated anti-β3 mAb AP3. Binding activity is presented as the percentage of the mean fluorescence intensity (MFI) of fibrinogen or fibronectin staining after background subtraction of the staining in the presence of EDTA, relative to the MFI of the AP3 staining.

CELL ADHESION ASSAYS

Cell adhesion on immobilized human fibrinogen was assessed by the measurement of cellular lactate dehydrogenase (LDH) activity as previously described [Zhu et al., 2007]. Briefly, cells suspended in HBS supplemented with 5.5 mM glucose, 1% BSA, and 1 mM Ca^{2+} were added into flat bottom 12-well plates (1×10^5 cells/well) precoated with 20 μg/ml fibrinogen and blocked with 1% BSA. After incubation at 37°C for 30 min, wells were washed three times with HBS supplemented as indicated above. Remaining adherent cells were lysed with 1% Triton X-100, and LDH activity was assayed using the Cytotoxicity Detection Kit (Roche Applied Science) according to the manufacturer's instructions. Cell adhesion was expressed as a percentage of bound cells relative to total input cells.

CELL SPREADING AND MICROSCOPY

Glass bottom six-well plates (MatTek Corporation, Ashland, MA) were coated with 20 μg/ml human fibrinogen in phosphate-buffered saline at pH 7.4 (PBS) overnight at 4°C, and then blocked with 1% BSA at RT for 1 h. The transiently transfected HEK293T cells were detached with trypsin/EDTA, washed three times with DMEM, and seeded on fibrinogen-coated plates. After incubation at 37°C for 1 h, cells were washed three times with PBS and fixed with 3.7% formaldehyde in PBS at RT for 10 min for microscopy.

Differential interference contrast (DIC) imaging was conducted on a Leica TCS SP2 spectral confocal system coupled to a DM IRE2 inverted microscope with a 63× oil objective. For the quantification of cell spreading area, outlines of 100 randomly selected adherent

cells were generated, and the area (μm^2) contained within each of these regions was measured using ImageJ software (Bethesda, MA).

RESULTS

DESIGN AND EXPRESSION OF MUTANT αVβ3 INTEGRINS

The crystal structures of the unliganded αXβ2 and αIIbβ3 [Zhu et al., 2008; Xie et al., 2010] and liganded αVβ3 and αIIbβ3 [Xiong et al., 2002; Xiao et al., 2004] show an important variation in one residue associated with the MIDAS, namely the β3 Ala^{252} and β2 Asp^{243}, respectively. This β3 Ala^{252} does not contribute to the Mg^{2+} binding in the MIDAS and consequently does not affect ligand binding, whereas the β2 Asp^{243} appears to contribute negative charge to the MIDAS that may affect ligand binding in the αXβ2 [Xie et al., 2010; Raborn et al., 2011]. We designed the A252D mutant, along with a single and a double ADMIDAS mutant, in the β3 subunit of the αVβ3. In addition, a glycosylation point mutation was created in the αV Calf-2 domain, αV_E781N/R783T (denoted α^*), which is expected to result in N-glycosylation of αV N781 to disrupt the αβ leg association and cause full activation of the αVβ3 integrin, as based on previous reports with the αIIbβ3 [Wang et al., 2010; Raborn et al., 2011]. To determine the expression of integrins on the cell surface, the WT, and αVβ3 mutants were transfected into HEK293T cells and subjected to immunostaining flow cytometry. The monoclonal antibody 10E5, which binds to the αIIb β-propeller domain, was used to detect the presence of any endogenous αIIb or β3 in HEK293T cell lines. When the WT and mutant αVβ3 integrins were cotransfected, 10E5 did not bind to the cells (Fig. 1), confirming that no endogenous αIIb was expressed. Three other monoclonal antibodies that bind to αVβ3 were used to detect integrin expression: AP3 recognizes the β3 hybrid domain, 7E3 binds to the β3 I domain, and LM609 binds to the αV β-propeller domain. WT and mutant αVβ3 integrins bound to all three of these antibodies with similar levels (Fig. 1), suggesting that all mutations have little effect on protein expression on the cell surface.

REGULATION OF FIBRINOGEN AND FIBRONECTIN BINDING BY THE β I MUTATIONS

Two-color flow cytometry was used to determine the fibrinogen and fibronectin binding of the WT and mutants. Under physiological Ca^{2+} conditions, the αVβ3 WT bound little fibrinogen or fibronectin. However, the WT bound fibrinogen and fibronectin with higher affinity in Mn^{2+} conditions (Fig. 2). The α^* glycosylation mutant showed four times the binding affinity to both fibrinogen and fibronectin in Ca^{2+} conditions and a twofold increase to both ligands in Mn^{2+} conditions compared to the WT (Fig. 2). Moreover, Mn^{2+} could not further activate this mutant for ligand binding, indicating this glycosylation mutant fully activates integrins. Although lower than the αVβ3 WT in both conditions, the ADMIDAS single and double mutants (D127A and D126A/D127A, respectively) bound at similar low levels to both fibrinogen and fibronectin in the presence of Ca^{2+}, but the D127A mutant bound ligands better than the D126A/D127A in Mn^{2+} conditions (Fig. 2), suggesting that both mutants have a varying loss of ADMIDAS function. When the D127A ADMIDAS mutant was combined with the α^* mutation, this α^*/D127A mutant showed near maximal affinity for both ligands in both Ca^{2+} and Mn^{2+} conditions (Fig. 2). When the α^* mutant was combined with the D126A/D127A mutant, this α^*/D126A/D127A mutant showed slightly lower binding to both ligands in Ca^{2+} and Mn^{2+} conditions compared to the α^*/D127A mutant but much better ligand binding than the ADMIDAS double mutant alone.

Compared to the WT, the MIDAS associated mutant A252D bound slightly less to fibrinogen and fibronectin in Ca^{2+} or Mn^{2+} conditions, but Mn^{2+} could increase the ligand binding of this mutant (Fig. 2). The results suggest that the increased negative charge from the Asp to the MIDAS ion reduces the ligand binding ability of the αVβ3 integrin. Combined with the glycosylation mutant, the α^*/A252D mutant showed similar affinity for fibrinogen and slightly lower affinity for fibronectin in Ca^{2+} conditions compared to the α^* mutant (Fig. 2), while this mutant showed the same affinity for both ligands in Mn^{2+} conditions. Overall, this α^*/A252D mutant shows maximal affinity for ligands, suggesting that shifting the integrin toward a more extended conformation by glycosylation could restore the ligand binding affinity reduced by the increased negativity in the MIDAS by the Asp carboxyl. When this A252D mutant was paired with the D127A ADMIDAS mutant, this double mutant showed slightly increased ligand binding affinity for both fibrinogen and fibronectin compared to the WT, D127A, and A252D mutants in Ca^{2+} conditions (Fig. 2), suggesting this mutant compensates for the added negative charge in the MIDAS and the loss of Ca^{2+} in the ADMIDAS. The α^*/A252D/D127A mutant showed similar binding levels to fibrinogen and fibronectin as the α^*/A252D mutant and higher levels of binding to both ligands than the α^*/D127A mutant in both conditions (Fig. 2). However, when the A252D mutant was combined with the D126A/D127A mutant, this mutant showed similar binding levels to fibrinogen and fibronectin as the D126A/D127A double mutant in both Ca^{2+} and Mn^{2+} conditions, implying this mutant also has abolished ADMIDAS function (Fig. 2). The α^*/A252D/D126A/D127A mutant bound fibrinogen and fibronectin with slightly higher affinity than the α^*/D126A/D127A mutant but lower than maximal binding affinity showed by the α^*/A252D mutant (Fig. 2), suggesting that the extended conformation is able to partially restore the ligand binding ability reduced due to the loss of ADMIDAS function.

EFFECTS OF MIDAS-ASSOCIATED RESIDUE ON ADHESION AND SPREADING

Using cytotoxicity detection of LDH, the percentage of adherent cells to immobilized fibrinogen was calculated by ratio of adherent cells to the total input cells. About 40% of the WT cells adhered to the immobilized fibrinogen (Fig. 3A), while the α^* mutant showed slightly increased adhesion. The ADMIDAS mutant D127A showed reduced adhesion, whereas the D126A/D127A mutant nearly abolished adhesion (Fig. 3A), which correlated to their reduced ligand binding and loss of ADMIDAS function. Interestingly, the adhesion ability of the D127A and D126A/D127A mutants was restored to levels near the WT when combined with the glycosylation mutation (Fig. 3A). The adhesion of the MIDAS associated mutant A252D was about 60% of the WT, while the α^*/A252D mutant showed slightly lower adhesion than the glycosylation mutant alone (Fig. 3A). Intriguingly, the A252D/D127A mutant

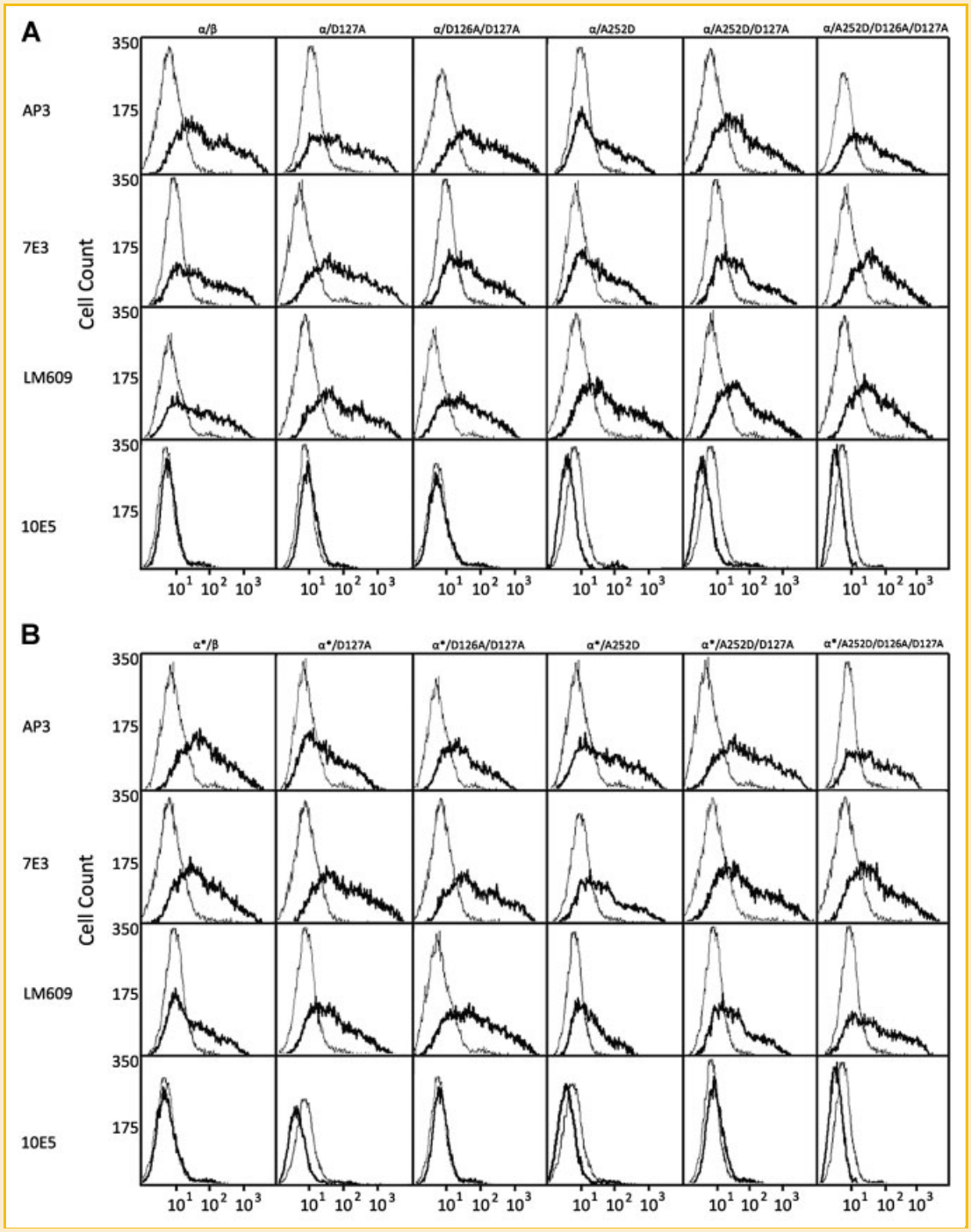

Fig. 1. Expression of WT and mutant αIIbβ3 integrins. Using immunofluorescent flow cytometry, HEK293T transfectants were labeled with AP3 (anti-β3), 7E3 (anti-β3), LM609 (anti-αV), and 10E5 (anti-αIIb). Thick and thin lines show labeling of the αVβ3 transfectant and the mock transfectant, respectively. A: Transfectants of the β subunit WT or mutations with the WT α subunit. B: Transfectants of the β subunit WT or mutations with the glycosylated α subunit.

showed slightly lower adhesion than the WT but increased adhesion compared to the A252D mutant alone, which related to the higher ligand binding ability of this double mutant than the A252D mutant. The α^*/A252D/D127A mutant showed similar adhesion as the α^* mutant and slightly higher adhesion than the α^*/A252D mutant (Fig. 3A). The A252D/D126A/D127A triple mutant also showed nearly abolished adhesion, similar to the D126A/D127A mutant, but when paired with the glycosylation mutation, the adhesion ability was recovered close to the adhesion level of the α^*/D126A/D127A mutant (Fig. 3A).

To determine if the MIDAS-associated residue and integrin conformation affect outside-in signaling, HEK293T transient

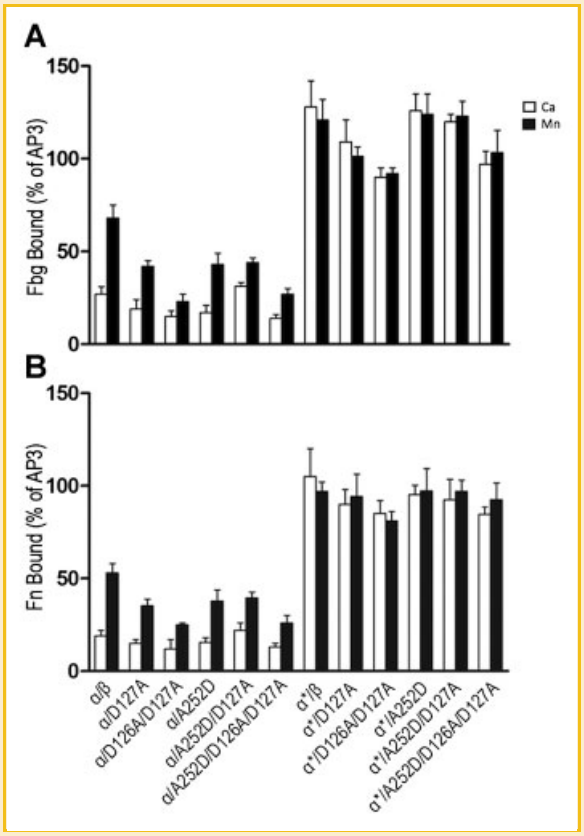

Fig. 2. Soluble ligand binding with fibrinogen and fibronectin. Cells were incubated with (A) FITC-fibrinogen in the presence of 5 mM Ca^{2+} or 1 mM Mn^{2+}, or (B) FITC-fibronectin in the presence of 5 mM Ca^{2+} or 1 mM Mn^{2+} as indicated. Binding activities were determined by flow cytometry and expressed as described in "Materials and Methods" Section. Error bars are standard deviation (SD). A *t*-test comparing the WT αβ to the D127A, D126A/D127A, A252D, A252D/D127A, and the A252D/D126A/D127A mutants individually for both Ca^{2+} and Mn^{2+} conditions showed that all were statistically significant except the A252D/D127A mutant in Ca^{2+} conditions.

transfectants were coated on immobilized fibrinogen at 37°C for 1 h, followed by fixation and microscopic analysis to determine cell spreading of the mutants. WT transfected cells exhibited normal adhesion and spreading (Fig. 3B), and the α* mutant exhibited similar spreading to the WT. The ADMIDAS D127A mutant adhered but did not spread. Moreover, the ADMIDAS D126A/D127A double mutant abolished spreading. The spreading ability of both ADMIDAS mutants was restored to slightly lower levels than the WT by the glycosylation mutation (Fig. 3B). The A252D mutant reported cell spreading similar to the WT, suggesting that despite the reduced ligand binding affinity and adhesion ability, the MIDAS associated residue does not appear to affect outside-in signaling. Consequently, the α*/A252D mutant showed similar spreading ability to the A252D mutant (Fig. 3C). The A252D/D127A mutant, although able to bind ligands and adhere, underwent slight spreading (Fig. 3C). The exact mechanism of this slight spreading remains elusive due to the uncertainty and intricacy of these mutant structures. The α*/A252D/D127A mutant shows restored spreading ability similar to the α*/D127A mutant probably due to the extended conformation with two separated legs. Finally, the A252D/D126A/D127A mutant showed abolished outside-in spreading ability, but when paired with the glycosylation mutation, this α*/A252D/D126A/D127A mutant restored the outside-in signaling ability leading to cell spreading (Fig. 3B).

DISCUSSION

Here we studied the effects of mutations of the ADMIDAS and the MIDAS-associated residue on ligand binding and signaling in the αVβ3 integrin. The ADMIDAS mutations decreased αVβ3 ligand binding. By mutating the β3 MIDAS associated residue Ala^{252} to Asp, the ligand binding affinity and adhesion ability decreased but had no effect on outside-in signaling. The variation in this residue among integrins appears to induce physiological differences in ligand binding and adhesion. When this mutant was combined with the ADMIDAS D127A mutant, the mutant reported an increase in ligand binding and adhesion but impaired spreading. While if more than one ADMIDAS residue was mutated, the ligand binding and adhesion ability were nearly abolished. However, the N-glycosylation and subsequent separation of the integrin legs brought on by the α* mutant was able to enhance and restore the ligand binding and signaling ability of the MIDAS-associated mutant, ADMIDAS mutants, and combinations of the two.

According to the crystal structure of the unliganded αIIbβ3 [Zhu et al., 2008] and liganded αIIbβ3 and αVβ3 [Xiong et al., 2002; Xiao et al., 2004], this Ala^{252} does not associate with the MIDAS metal ion and does not affect ligand binding (Fig. 4A). However, the integrins αLβ2 and α4β7 both contain an Asp residue instead of an Ala in the corresponding position. In the crystal structure of the unliganded αXβ2 [Xie et al., 2010], this Asp side chain points toward the MIDAS ion and obviously increases the negativity of the MIDAS, which can reduce its ligand binding affinity by repelling the negatively charged residue in the ligand that associates with the MIDAS Mg^{2+} ion. In our study, we mutated the β3 residue Ala^{252} to Asp (Fig. 4B). This αVβ3 mutant showed lower binding affinity and did not strongly adhere to immobilized ligands, similar to the WT α4β7 and αLβ2 integrins [Chen et al., 2003, 2004, 2006]. Although ligand binding and adhesion were reduced, this mutant showed similar outside-in signaling capability to the WT αVβ3, allowing the cell to spread on immobilized ligands. Nevertheless, when the activating α* glycosylation mutation was introduced in conjunction with this A252D mutant, the conformation of the leg separation restored the ligand binding affinity and adhesion ability to near maximal affinity. Thus, our data confirmed our hypothesis that αVβ3 WT containing Ala has higher ligand binding affinity than the A252D mutant, and it suggests that the corresponding Asp residue in the α4β7 and αLβ2 integrins decreases ligand-binding affinity.

In normal physiological conditions, α4β7 and αLβ2 integrins mediate cell rolling and firm adhesion, while α2β1, α5β1, and αVβ3 integrins mediate only firm adhesion [Butler et al., 2002; McEver and Zhu, 2010]. Interestingly, when one of the ADMIDAS residues is mutated in these integrins, the α4β7 and αLβ2 mutants increase ligand binding, whereas the α2β1, α5β1, αIIbβ3, and now αVβ3

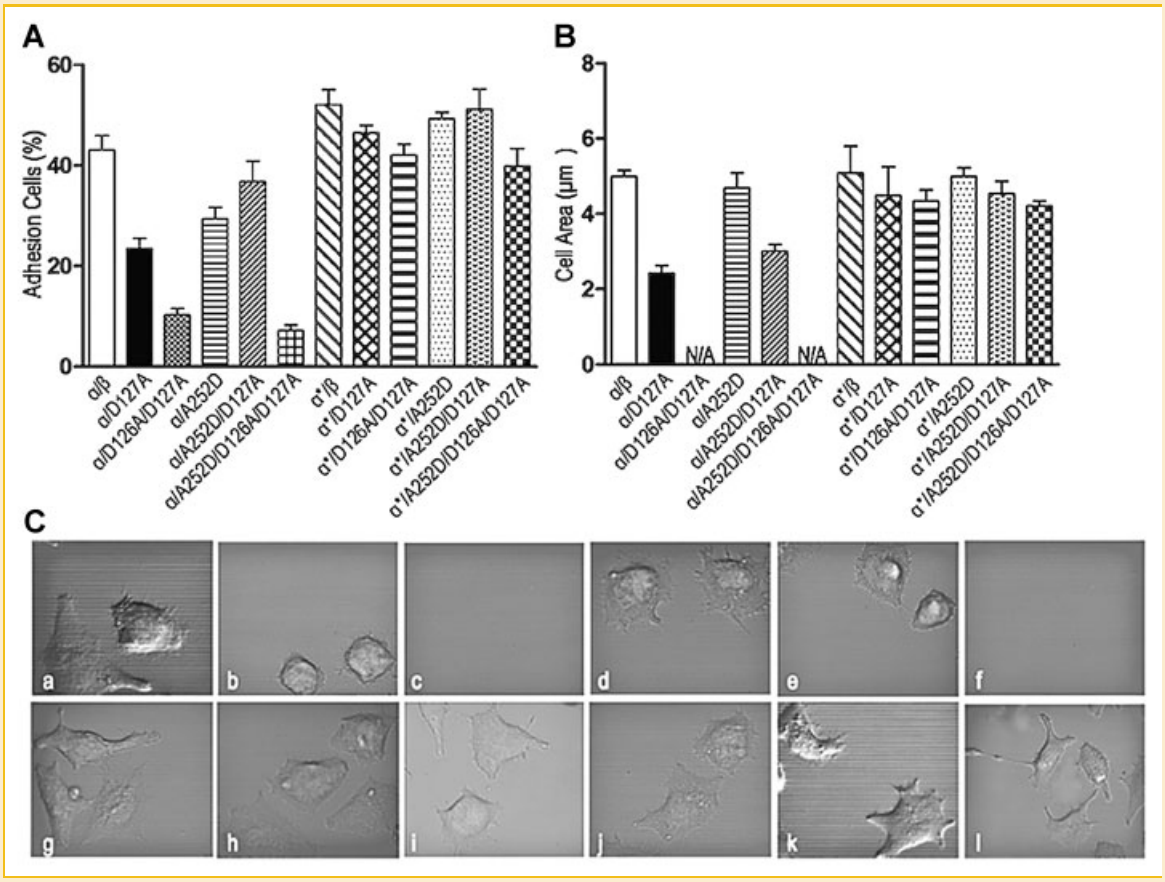

Fig. 3. Cell adhesion and spreading. A: Adhesion of HEK293T transfectants to surfaces coated with 20 μg/ml fibrinogen. The amount of bound cells was determined by measuring LDH activity as described in "Materials and Methods" Section. Data are representative of three independent experiments, each in triplicate. B: Quantification of the areas of adhering/spreading cells as described in "Materials and Methods" Section. Error bars are SD. C: DIC images of HEK293T transfectants after adhering to immobilized fibrinogen at 37°C. a: αβ; b: D127A; c: D126A/D127A; d: A252D; e: A252D/D127A; f: A252D/D126A/D127A; g: α*β; h: α*/D127A; i: α*/D126A/D127A; j: α*/A252D; k: α*/A252D/D127A; l: α*/A252D/D126A/D127A. The images are representatives of three independent experiments.

mutants decrease ligand binding [Chen et al., 2003, 2004, 2006; Mould et al., 2003a; Valdramidou et al., 2008; Raborn et al., 2011]. Our results suggest that the MIDAS-associated residue contributes to these differences. In β2 and β7 integrin subunits, the MIDAS associated residue is Asp, while in β1 and β3 integrin subunits, the corresponding residue is Ala. Comparing the crystal structures of the closed [Zhu et al., 2008] and open [Xiao et al., 2004] headpiece conformation of the αIIbβ3, the Asp shifts 0.7 Å from coordinating with the MIDAS metal ion in the closed headpiece to associating with the ADMIDAS Ca^{2+} ion in the open headpiece. Consequently, the adjacent Ala^{252} residue also shifts away from the MIDAS and toward the ADMIDAS ion. In this open headpiece conformation, the Ala, a nonpolar amino acid, does not coordinate with the ADMIDAS Ca^{2+} ion. Therefore, in the α2β1, α5β1, and αVβ3 integrins with this Ala residue, mutation of even one ADMIDAS residue leads to loss of coordination with its Ca^{2+} ion that results in a loss of ADMIDAS function with lower ligand binding compared to the respective WT. Conversely, when αVβ3 Ala^{252} is mutated to Asp and one of the ADMIDAS residues is mutated, the Asp^{252} shifts toward the ADMIDAS and, along with the Asp^{251}, may be able to coordinate and retain the Ca^{2+} ion (Fig. 4C). Since the ADMIDAS function is preserved and the negative Asp^{252} shifts away from the MIDAS, the ADMIDAS ion stabilizes the open conformation and the MIDAS ion is able to associate with ligands at a higher affinity than the A252D mutant alone (Fig. 4C) but with reduced outside-in signaling. However, if both ADMIDAS residues were mutated along with the β3 A252D mutation, this mutant experienced a drastic reduction in ligand binding affinity and adhesion because the ADMIDAS function was abolished due to the loss of the ADMIDAS Ca^{2+} ion (Fig. 4D). In β2 and β7 integrin subunits, the corresponding residue is Asp instead of Ala in β3. Therefore, with single ADMIDAS mutations [Chen et al., 2003, 2004, 2006], the MIDAS-associated residue Asp may coordinate and retain the ADMIDAS Ca^{2+} ion and allow the integrin to bind ligands and adhere with higher affinity than the WT β2 and β7 integrins. We propose that if both ADMIDAS residues are mutated, the β2 and β7 integrins are unable to retain the ADMIDAS Ca^{2+} ion and thus eliminate the function of the ADMIDAS, resulting in loss of ligand binding. Further experiments are necessary to confirm this hypothesis.

When the αVβ3 integrin was induced by glycosylation to undergo a conformational change that separated the two legs, all ADMIDAS, and MIDAS-associated residue mutants showed restored

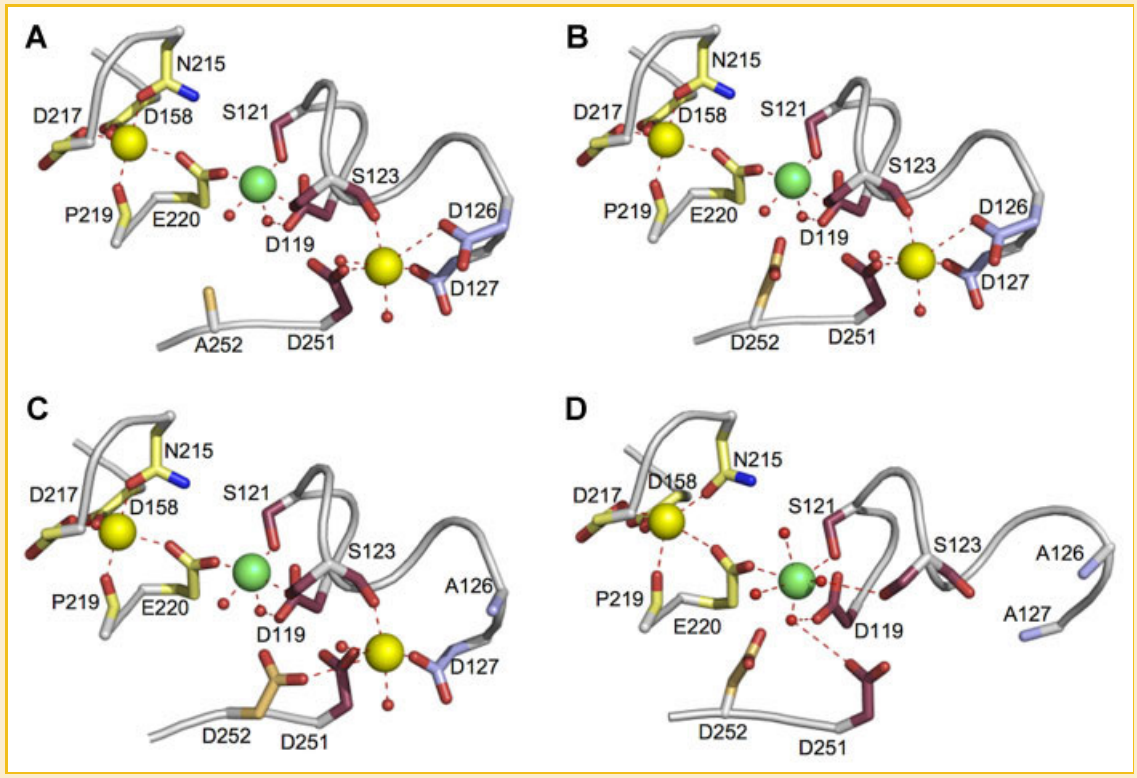

Fig. 4. WT and simulated mutant αIIbβ3 integrin structures of the metal-binding sites. Structure of liganded open headpiece (A) WT metal-binding sites (PDB Code: 3FCU) (Xiao et al., 2004). Simulated β3 mutant metal-binding sites with point mutations in the liganded open headpiece (B) A252D and (C) A252D/D126A, which was formed by leaving the backbone untouched and shifting the Asp^{252} side chain roughly 45° toward the ADMIDAS Ca^{2+} ion, and (D) A252D/D126A/D127A, which was made from the unliganded closed headpiece (PDB Code: 3FCS) without the ADMIDAS Ca^{2+} that is consistent with our results. The metal-binding sites are colored as follows: raspberry, MIDAS; pale yellow, SyMBS; light blue, ADMIDAS; and light orange, MIDAS-associated residue Asp or Ala. N and O atoms involved in metal coordinating side chains or carbonyl backbones are colored in blue and red, respectively. Ca^{2+} and Mg^{2+} ions are colored in yellow and green, respectively. Polar coordination between O atoms and metal ions are shown by dashed red lines.

ligand binding and signaling. This confirms the necessity of the integrin to adopt a conformation with two separated legs and TM domains to undergo signal transduction as previous observed [Zhu et al., 2007; Wang and BH, 2010; Wang et al., 2010; Raborn et al., 2011].

ACKNOWLEDGMENTS

Grants: We thank the American Heart Association (#10GRNT3960011) and the Louisiana Board of Regents (LEQSF(2009-12)-RD-A07) for financial support.

REFERENCES

Bajt ML, Loftus JC. 1994. Mutation of a ligand binding domain of b3 integrin: Integral role of oxygenated residues in aIIbb3 (GPIIb-IIIa) receptor function. J Biol Chem 269:20913–20919.

Butler B, Williams MP, Blystone SD. 2002. Ligand-dependent activation of integrin αvβ3. J Biol Chem 278:5264–5270.

Chen JF, Salas A, Springer TA. 2003. Bistable regulation of integrin adhesiveness by a bipolar metal ion cluster. Nat Struct Biol 10:995–1001.

Chen JF, Takagi J, Xie C, Xiao T, Luo BH, Springer TA. 2004. The relative influence of metal ion binding sites in the I-like domain and the interface with the hybrid domain on rolling and firm adhesion by integrin a4b7. J Biol Chem 279:55556–55561.

Chen JF, Yang W, Kim M, Carman CV, Springer TA. 2006. Regulation of outside-in signaling by the b2 I domain of integrin aLb2. Proc Natl Acad Sci USA 103:13062–13067.

Goodman TG, Bajt ML. 1996. Identifying the putative metal ion-dependent adhesion site in the b2 (CD18) subunit required for a_Lb_2 and aMb_2 ligand interactions. J Biol Chem 271:23729–23736.

Harding MM. 2001. Geometry of metal–ligand interactions in proteins. Acta Crystallogr D Biol Crystallogr 57:401–411.

Hynes RO. 2002. Integrins: Bi-directional, allosteric, signalling machines. Cell 110:673–687.

Hynes RO, Zhao Q. 2000. The evolution of cell adhesion. J Cell Biol 150: F89–F96.

Kamata T, Tieu KK, Tarui T, Puzon-McLaughlin W, Hogg N, Takada Y. 2002. The role of the CPNKEKEC sequence in the beta(2) subunit I domain in regulation of integrin alpha(L)beta(2) (LFA-1). J Immunol 168:2296–2301.

Lee JO, Rieu P, Arnaout MA, Liddington R. 1995. Crystal structure of the A domain from the a subunit of integrin CR3 (CD11b/CD18). Cell 80:631–638.

Lin ECK, Ratnikov BI, Tsai PM, Gonzalez ER, McDonald S, Pelletier AJ, Smith JW. 1997. Evidence that the integrin b3 and b5 subunits contain a metal ion-

dependent adhesion site-like motif but lack an I domain. J Biol Chem 272: 14236–14243.

Loftus JC, O'Toole TE, Plow EF, Glass A, Frelinger AL III, Ginsberg MH. 1990. A b_3 integrin mutation abolishes ligand binding and alters divalent cation-dependent conformation. Science 249:915–918.

Luo BH, Springer TA, Takagi J. 2003. Stabilizing the open conformation of the integrin headpiece with a glycan wedge increases affinity for ligand. Proc Natl Acad Sci USA 100:2403–2408.

Luo BH, Takagi J, Springer TA. 2004. Locking the b3 integrin I-like domain into high and low affinity conformations with disulfides. J Biol Chem 279:10215–10221.

Luo BH, Carman CV, Springer TA. 2007. Structural basis of integrin regulation and signaling. Annu Rev Immunol 25:619–647.

Luo BH, Karanicolas J, Harmacek LD, Baker D, Springer TA. 2009. Rationally designed integrin b3 mutants stabilized in the high affinity conformation. J Biol Chem 284:3917–3924.

McEver R, Zhu C. 2010. Rolling cell adhesion. Ann Rev Cell Dev Biol 26: 363–396.

Mould AP, Akiyama SK, Humphries MJ. 1995. Regulation of integrin a5b1-fibronectin interactions by divalent cations. J Biol Chem 270:26270–26277.

Mould AP, Barton SJ, Askari JA, Craig SE, Humphries MJ. 2003a. Role of ADMIDAS cation-binding site in ligand recognition by integrin a5b1. J Biol Chem 278:51622–51629.

Mould AP, Symonds EJ, Buckley PA, Grossmann JG, McEwan PA, Barton SJ, Askari JA, Craig SE, Bella J, Humphries MJ. 2003b. Structure of an integrin-ligand complex deduced from solution X-ray scattering and site-directed mutagenesis. J Biol Chem 278:39993–39999.

Murcia M, Jirouskova M, Jihong L, Coller BS, Filizola M. 2008. Functional and computational studies of the ligand-associated metal binding site of β3 integrins. Proteins 71:1779–1791.

Raborn J, Wang W, Luo B. 2011. Regulation of integrin αIIbβ3 ligand binding and signaling by the metal ion binding sites in the β I domain. Biochemistry 50:2084–2091.

Salas A, Shimaoka M, Kogan AN, Harwood C, von Andrian UH, Springer TA. 2004. Rolling adhesion through an extended conformation of integrin aLb2 and relation to a I and b I-like domain interaction. Immunity 20:393–406.

Shimaoka M, Takagi J, Springer TA. 2002. Conformational regulation of integrin structure and function. Annu Rev Biophys Biomol Struct 31:485–516.

Shimaoka M, Xiao T, Liu J-H, Yang Y, Dong Y, Jun C-D, McCormack A, Zhang R, Joachimiak A, Takagi J, Wang J-h, Springer TA. 2003. Structures of the aL I domain and its complex with ICAM-1 reveal a shape-shifting pathway for integrin regulation. Cell 112:99–111.

Takagi J, Petre BM, Walz T, Springer TA. 2002. Global conformational rearrangements in integrin extracellular domains in outside-in and inside-out signaling. Cell 110:599–611.

Takagi J, Strokovich K, Springer TA, Walz T. 2003. Structure of integrin a5b1 in complex with fibronectin. EMBO J 22:4607–4615.

Tozer EC, Liddington RC, Sutcliffe MJ, Smeeton AH, Loftus JC. 1996. Ligand binding to integrin a_{IIb}b3 is dependent on a MIDAS-like domain in the b3 subunit. J Biol Chem 271:21978–21984.

Valdramidou D, Humphries MJ, Mould AP. 2008. Distinct roles of β1 metal ion-dependent adhesion site (MIDAS), adjacent to MIDAS (ADMIDAS), and ligand-associated metal-binding site (LIMBS) cation-binding sites in ligand recognition by integrin α2β1. J Biol Chem 283:32704–32714.

Wang W, Luo BH. 2010. Structural basis of integrin transmembrane activation. J Cell Biochem 109:447–452.

Wang W, Fu G, Luo BH. 2010. Dissociation of the α-subunit calf-2 domain and the β-subunit I-EGF4 domain in integrin activation and signaling. Biochemistry 49:10158–10165.

Whittaker CA, Hynes RO. 2002. Essay from the genome annotation series: Distribution and evolution of the von Willebrand/Integrin A domain: A widely dispersed domain with roles in cell adhesion and elsewhere. Mol Biol Cell 13:3369–3387.

Xiao T, Takagi J, Wang J-h, Coller BS, Springer TA. 2004. Structural basis for allostery in integrins and binding of fibrinogen-mimetic therapeutics. Nature 432:59–67.

Xie C, Zhu J, Chen X, Mi L, Nishida N, Springer TA. 2010. Structure of an integrin with an alphaI domain, complement receptor type 4. EMBO J 29:666–679.

Xiong JP, Stehle T, Diefenbach B, Zhang R, Dunker R, Scott DL, Joachimiak A, Goodman SL, Arnaout MA. 2001. Crystal structure of the extracellular segment of integrin aVb3. Science 294:339–345.

Xiong JP, Stehle T, Zhang R, Joachimiak A, Frech M, Goodman SL, Arnaout MA. 2002. Crystal structure of the extracellular segment of integrin aVb3 in complex with an Arg-Gly-Asp ligand. Science 296:151–155.

Yang W, Shimaoka M, Chen JF, Springer TA. 2004. Activation of integrin b subunit I-like domains by one-turn C-terminal a-helix deletions. Proc Natl Acad Sci USA 101:2333–2338.

Zhu J, Carman CV, Kim M, Shimaoka M, Springer TA, Luo BH. 2007. Requirement of α and β subunit transmembrane helix separation for integrin outside-in signaling. Blood 110:2475–2483.

Zhu J, Luo BH, Xiao T, Zhang C, Nishida N, Springer TA. 2008. Structure of a complete integrin ectodomain in a physiologic resting state and activation and deactivation by applied forces. Mol Cell 32:849–861.